Studies of the Thermodynamic Conditions for the Existence of a Stable Liquid Phase in Square Well Fluids

Nasir M. Tukur
Chemical Engineering Department
King Fahd University of Petroleum & Minerals
Dhahran 31261, Saudi Arabia
e-mail: nmtukur@kfupm.edu.sa

Leslie V. Woodcock
Department of Chemistry, University of Manchester Institute of Science and Technology, Manchester, UK
e-mail: Les.Woodcock@umist.ac.uk

and Leo Lue
Department of Chemical Engineering, University of Manchester Institute of Science and Technology, Manchester, UK
e-mail: leo.lue@umist.ac.uk

ABSTRACT

The condition under which certain systems may not have a stable liquid phase, instead, sublime from the solid to the vapor phase has been the subject of investigations by many. Until recently, it used to be thought that any amount of attraction added to a short ranged repulsion would give rise to a liquid phase. However, computer simulations, theoretical, as well as experimental studies have showed that this is not the case.

By use of Hyper-parallel tempering Monte Carlo (HPTMC) simulation, computer simulations were performed to obtain the liquid-vapor co-existence data for square-well (SW) fluid with variable interaction range with the view of determining the conditions where the liquid state will simply squeeze out. The interaction range (λ) which plays a significant role in giving rise to a liquid phase in the phase diagram was varied from 1.21 to 3.0.

The results of the work clearly indicate that the range of temperatures for which the liquid is stable shrinks as the interaction range decreases. And for sufficiently short interaction ranges, the square-well fluid has no stable liquid phase with a threshold value of λ = 1.24.

1. INTRODUCTION

Understanding the phase behaviour of fluids & fluid mixtures is an important subject for design of chemical engineering processes such as Absorption, Distillation and Extraction. This is because very many chemical engineering activities involve the formation and contact of different phases. In mixtures for example, vapor-liquid equilibrium calculations can establish the compositions of vapor and liquid phases coexisting with each other (as happens when a mixture is boiled), and so this sort of information is ultimately used to design distillation columns, boilers and condensers in chemical plants. The tremendous capital involved in

collecting experimental data of true phase co-existence has served to make thermodynamic properties prediction an ongoing focus of fundamental chemical engineering research. In certain instances, it may be necessary to prevent the formation of new phases such as in the design of gas pipeline systems where the occurrence of significant amounts of liquid phase could block the pipeline with possibly disastrous consequences. Whatever the application however, knowledge of thermodynamics of fluids under various conditions is needed by engineers.

Although there have been tremendous advances in liquid state physics, the conditions that are necessary for the liquid state to occur have received less attention from investigators. Existence of a liquid state implies, having a critical point in the phase diagram. It is a general knowledge that pure hard sphere system does not have a critical point in its phase diagram, which indicates the absence of a liquid state. It has, however, been widely believed that any amount of attractive interaction added to the repulsive hard-core will give rise to a liquid state. But recent theoretical studies as well as experimental studies on colloid-polymer mixtures [1,2,3] suggest very strongly that an attractive potential of sufficient long range is in fact necessary for the existence of the liquid state. In fact, lately it has become very clear that below a critical range of the attractive interaction the gas–liquid transition of a given substance becomes metastable with respect to the fluid–solid transition. This phenomenon was first noted in connection with phase transitions in mixed suspensions of colloidal particles and non-adsorbing polymer molecules by Gast, Hall, and Russell [4]. In such colloid–polymer mixtures, the range and the depth of the attractive interaction can be adjusted by the size and concentration of the added polymer molecules [5]. Experiments on model colloid polymer mixtures have provided conclusive evidence that the topology of the phase diagram is indeed determined by the ratio of the radius of gyration of the polymer molecules to the radius of the colloidal particles. [2 &3]

Following the work on colloid–polymer mixtures, it was subsequently recognized that sufficiently short-ranged attractions could also lead to gas–liquid metastability in molecular systems. An example of such a molecular system that has emerged in recent years is the C_{60} molecule. Hagen et al. [6] mapped out the phase diagram of C_{60} using computer simulations in which the C_{60} molecules are represented by spheres interacting via the Girifalco potential [7]. They concluded that C_{60} has no stable liquid phase. Cheng et al., [8] also starting from the Girifalco potential, used an integral equation approach combined with molecular dynamics simulations to establish the phase diagram of C_{60}. They predicted that the liquid phase is stable in a narrow range of temperatures and densities. Subsequent studies have not definitely settled the issue [9,10,11]. Altogether, these investigations seem to suggest that C_{60} is a borderline case which may or may not have a liquid phase. The example of C_{60} has led to several systematic studies, both theoretical and numerical to establish the relationship between the range of the attractive part of the intermolecular potential and the stability of the liquid phase [12-15]. These investigations confirmed that below a critical range of the attraction the liquid state becomes metastable.

For the case of solutions of globular proteins, it has been known for quite sometime that a liquid–liquid phase separation occurs below the fluid–solid transition, i.e., this liquid–liquid phase separation is metastable. Recently, it was realized that a possible explanation for the occurrence of this metastable liquid–liquid phase separation is again the fact that the range of attraction is small compared to the size of the protein molecule. [16]

All the above studies seem to suggest that an attractive potential of sufficiently long range is necessary for the existence of liquid phase. However, estimates for the value of the range of the attractions where this change occur differ. [9,15,17]

The goal of this research is to determine through molecular simulation the necessary and sufficient condition for a square-well potential to give rise to a (stable) liquid. The results will be contrasted with other reported theoretical results if available.

2. MODEL

The square-well (SW) interparticle potential has been used as a simplified model for modeling the behaviour of realistic fluids. This simplified potential captures both attractive and repulsive interactions with only three parameters. A square-well fluid composed of particles of diameter σ that interact with the potential

$$u(r) = \begin{cases} \infty & 0 < r < \sigma, \\ -\varepsilon, & \sigma \leqslant r < \lambda\sigma, \\ 0, & \lambda\sigma \leqslant r, \end{cases} \qquad (1)$$

where r is the interparticle distance, λ is the range of the well in units of the hard core diameter σ, and ε, the depth of the well. By varying the range of the SW fluid it is possible to have different systems represented by the SW ranging from hard sphere to van der Waals fluids [18].

Square-well fluids have been extensively studied in the past by statistical thermodynamics methods [19,20,21,22,23] and computer simulations [24,24,25,27], often with goal of obtaining the structural and thermodynamic properties of the square-well systems. Statistical mechanics research on the thermodynamic properties of the SW fluid started with the perturbation theory of Barker and Henderson [19]. The analytical results of the expansion about the hard sphere state provided the groundwork for much of thermodynamic perturbation theory. However, numerical solutions for the Percus-Yevick [20], hypernetted chain [21], and mean spherical approximation (MSA) [22] of the Ornstein-Zernike (OZ) all show that a non perturbative integral equation approach can provide very good estimates of the properties of the square-well system.

Monte Carlo and molecular dynamics simulation results were first reported by Rotenberg [24] and Alder *et al.* [25] for the case of $\lambda=1.5$. Simulations for other values of λ have been done by Rosenfeld and Thieberger [26], and Henderson et al. [27].

Of recent, large amount of Monte Carlo and molecular dynamics simulation data on the square-well fluid using various techniques have been published as well, mainly to explore the liquid-vapor co-existence. Vega *et al*. [18] used the Gibbs ensemble Monte Carlo technique (GEMC) to obtain the vapor-liquid phase equilibria of square-well fluids with potential ranges of $\lambda = 1.25, 1.375, 1.5, 1.75,$ and $2.$ They also determined the dependence of the critical constants on λ. The results of Vega *et al.* [18] seem to suggest that the SW fluid deviates from

the universal Ising behaviour for $\lambda = 2$. However, their results differ from studies reported later. de Miguel [28] for example, confirmed the existence of Ising behaviour for the $\lambda = 2$ Square-well system using a mixed field finite-size scaling simulation within the grand canonical ensemble. The thermodynamic scaling Monte Carlo (TSMC) simulations by Brilliantov and Valleau [29], and grand canonical Monte Carlo (GCMC) calculations by Orkoulas and Panagiotopoulos [30] all lead to the conclusion that SW fluid follows universal Ising behaviour.

In their study of the square-well systems, Elliot and Hu [31] using molecular dynamics and isochoric integration also determined the vapor-liquid equilibrium and also reported vapour pressures in agreement with previous results of perturbation theory [23].

Kiselev *et al.* [32] in their study, performed extensive MD and MC simulations for square-well fluids over a range of values for λ, and subsequently came up with a crossover equation of state (EOS) that yields the exact second and third virial coefficients, and accurately reproduces first-order perturbation theory results.

Del Rio *et al.* [33] using the so called 'hybrid simulation approach' determined the equilibrium between vapour and liquid in a square-well system with interaction ranges $\lambda = 1.25, 1.5, 1.75,$ and 2, by combining chemical potentials calculated via the Gibbs ensemble Monte Carlo (GEMC) with pressures calculated by *NVT* Monte Carlo method. The phase equilibrium was determined from the thermodynamic conditions of the equality of pressure and chemical potential in the two phases. The authors reported that their results of the hybrid approach are of much higher accuracy than those of conventional GEMC simulations [18]. They also found results in agreement with the previous reported results of perturbation theory.

Orea *et al*. [34] obtained the properties of the liquid-vapour interface of square-well fluids with ranges of interaction $\lambda = 1.5, 2.0, \& 3.0$ using MC simulations and square-gradient theories that combine Carnahan-Starling equation of state for hard spheres. Their results were in good agreement with the surface tension results reported by Singh, Kofke & Errington [35] obtained using grand canonical transition matrix Monte Carlo & Molecular Dynamics simulation.

The main purpose of this work is to investigate the effect of varying the range of attractive forces on the phase behaviour of square-well by varying the values of λ, the range of the well, from 1.2 to 3.0 using the hyper-parallel tempering simulation technique of Yang and de Pablo [36] as applied to grand canonical ensemble. Attempts will be made to identify the thermodynamic conditions where the liquid state may not be present.

To date, the authors are not aware of any systematic simulation study to find the boundary between stable and metastable liquid-vapor transitions for the square-well fluid. Neither is he aware of the use of hyper-parallel tempering Monte Carlo technique applied to square-well fluid. However, it should be mentioned that a rough estimate of the threshold value has been calculated theoretically to be $\lambda = 1.25$ using a simple van der Waals model [37,38] for both the fluid and the solid phases. A similar value of $\lambda = 1.25$ was found from simple cell model [39]. In both cases, the liquid phase disappears as a stable phase as a result of the lowering of the vapor-liquid critical temperature when λ was lowered.

2.1 Model Details

The range of the attractive intermolecular forces in square-well fluid is measured by the range of the well, λ. By changing the values of λ, one is able to observe the effect of the range of attractive forces on the phase behaviour of square-well and ultimately find the value of λ where the liquid phase just simply squeezes out. Figure 1 gives the potential energy as function of the interparticle distance.

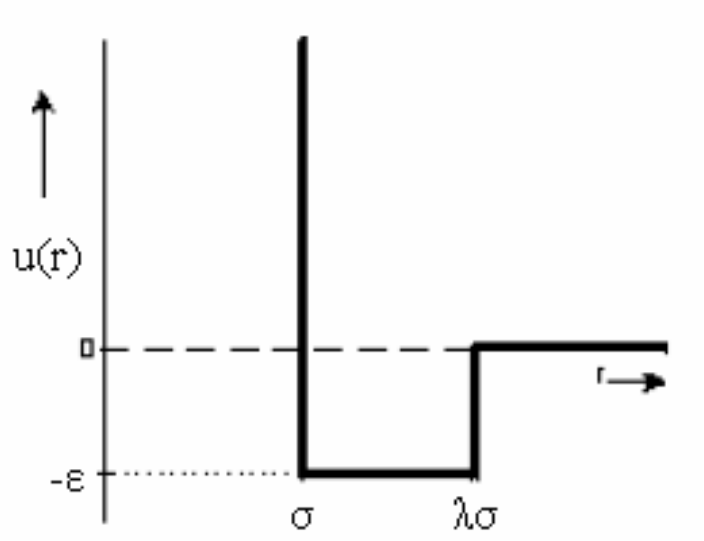

Figure 1: Illustration of the square-well potential

2.2 Simulation Details

In this work, the hyper-parallel tempering method of Yang and de Pablo [36] has been used in the grand canonical ensemble. This method is very effective in overcoming difficulties in molecular simulation particularly complex systems at low temperatures, where the configurations can get easily trapped in local energy minima, thereby precluding sampling of other relevant regions of phase space. The main feature in this technique is that neighbouring configurations can be swapped as the simulation proceeds. An overview of the method for grand canonical Monte Carlo (GCMC) as apply to one-component system has been given in Chapter 3. Only specific details are given below.

In any GCMC simulation, the simulation cell volume V, the temperature (T) or the inverse temperature, $\beta = 1/k_BT$ and the chemical potential (μ) are specified as input parameters to the simulation. The number of particles N and the total configurational energy E are allowed to fluctuate, the temperature and the chemical potential span the phase diagram, and by tuning their values, transitions can be induced between phases.

At the start of the simulation, the number of particles as well as the maximum number of particles to be used in the simulation is specified. About 512 particles are usually present at the start and 2048 is specified as the maximum. More than one test systems can be simulated at the same time, as such, about 10-12 test systems were simulated for each chosen range of the well.

In a typical MC cycle, the necessary input parameters are first defined. These are the max. # of particles, initial # of particles, # of systems under investigation, # of link cells, # of MC cycles, maximum displacement and the reduced volume (125-1000 depending on λ values*)*. Other parameters to be specified are the value of the range *(λ),* inverse temperature *(βε),* chemical potential *(βμ)* and the co-ordinates of the particle sites. The usual periodic boundary condition is then applied and then a check is made to ensure that there is no overlap of particles. Link cells are then set and initialized. The cell dimension has to be ensured that it is greater than the range of the well *($r_{cell} > \lambda$).* It was also ensured that the simulation box sizes are large compared with correlation length, by choosing the box length $L >> \sigma$ in accordance with ref. [100] to guarantee that the statistical properties obtained are reliable.

Standard Monte Carlo trial moves are used to locally update the configuration of each of the system. Standard Metropolis acceptance-rejection criteria are employed within each of the system under investigation. Fluctuations in the particle number occur by means of particle insertions and deletions. Similarly, the usual acceptance-rejection criteria in grand canonical ensemble are employed. Configuration swaps are also attempted in each cycle with probability as given in the original paper of Yang and de Pablo [36]. A total of 10^7 Monte Carlo steps are required to generate the grand canonical density distribution.

At sub-critical temperatures, the density distribution is characterized by a double peaked structure provided the chemical potential is close to the coexistence value. The determination of the precise location of a coexistence point is achieved by tuning the chemical potential at any given temperature until the areas under the two peaks become the same. The co-existing densities of the two co-existing phases then correspond to the mean densities under these peaks.

2.3 Pressure Determination

The discontinuity in the square-well potential makes it impossible to determine pressure directly from the simulation. Therefore, pressures corresponding to the co-existing phases (ρ_L & ρ_V) have been calculated using radial distribution function *g(r)* within virial equation. Since there is a discontinuity in the potential, it implies that there is also discontinuity in *g(r)* at the same separations(s). The pressure only depends on the value(s) of the radial distribution function at these discontinuities [40]. The equation to be used according to Heyes [40] is:

$$\frac{P\beta}{\rho} = 1 + \frac{2}{3}\pi\rho\sigma^3\left[g\left(\sigma^+\right) + \lambda^3 g\left(\lambda^-\sigma\right)\left(1-\exp\left(-\varepsilon\beta\right)\right)\right] \qquad (2)$$

where $g(\sigma^+)$ is the value of the radial distribution function at the limit of $r \rightarrow \sigma$ taken from right inwards, while $g(\lambda^-\sigma)$ is the value of the radial distribution function at the second discontinuity in the potential approached from the left.

2.4 Determination of Critical Points

Scaling laws will be utilized to evaluate the critical properties. The critical temperature is evaluated by fitting the calculated $\rho - T$ coexistence data according to the form of the equation [41]

$$\rho_l - \rho_g = b\left(T_c - T\right)^{\beta}$$

where $\beta \approx 0.325$ is the classical critical exponent (since Ising behaviour has been confirmed for these systems [29,30]), b and the critical temperature Tc are calculated from non-linear regression. Subsequently, the critical density ρ_C can be determined using non-linear regression based on the law of rectilinear diameters:

$$\frac{\rho_l + \rho_g}{2} = \rho_c + A\left(T - T_c\right)$$

where A and critical density ρ_C are calculated from the regression.

3. RESULTS AND DISCUSSIONS

Figures 2 to 7 show the frequency histogram of densities obtained using the hyper-parallel tempering technique implemented in the grand canonical ensemble for square-well fluids with potential ranges characterized by $\lambda = 1.25, 1.375, 1.5, 1.75, 2.0, 3.0$. Figures 8 to 13 present the temperature-density plots for the potential range of $\lambda = 1.25, 1.375, 1.5, 1.75, 2.0, 3.0$. Table 1 reports the critical properties of the SW fluid with variable range. Figures 14 to 16 give the lines of liquid-vapour phase coexistence in μ*-T* space. Figure 17 shows the vapour-liquid coexistence lines with temperatures scaled with the critical T_C. Figures 18 to 22 are results for the square-well fluids with $\lambda = 1.21\text{-}1.24$.

The discussion of results will be subdivided into two sections. The first section will be for λ = 1.25 to 3.0. This range has been the subject of investigation by many authors [29,30,31,32,33]. Liquid-vapour transition has been observed in this range of λ. The second section will be for λ = 1.21-1.24.

λ = 1.25 to 3.0

The frequency histogram of densities presented in Figures 2 to 7 are determined using the hyper-parallel tempering technique implemented in the grand canonical ensemble for square-well fluids with potential ranges characterized by $\lambda = 1.25, 1.375, 1.5, 1.75, 2.0, 3.0$. It is clear from these figures that for the chosen temperature and chemical potential, the system samples configurations of two stable states corresponding to the co-existing vapour and liquid phases. The normal conversions were adopted for the reduced density ($\rho^* = \rho\,\sigma^3$), temperature ($T^* = k_B\,T\,\varepsilon^{-1}$), and pressure ($P^* = P\sigma^3\,\varepsilon^{-1}$).

The coexisting vapor-liquid temperature-density coexistence curves for the SW fluids are compared in Figs. 8 to 13 with previous reported results obtained with the GEMC method [18] and those obtained by the so-called hybrid simulation approach [33]. It can be seen from the figures, our densities are generally closer to those reported by Del Rio *et al.* [33] which were calculated using the new hybrid approach than the earlier reported values of Vega *et al.* [18], except for λ = 1.75 (T*=1.73) where the difference is a bit high. The results of this work are in complete agreement with those reported by Orkoulas et al. [30] for λ = 3.00.

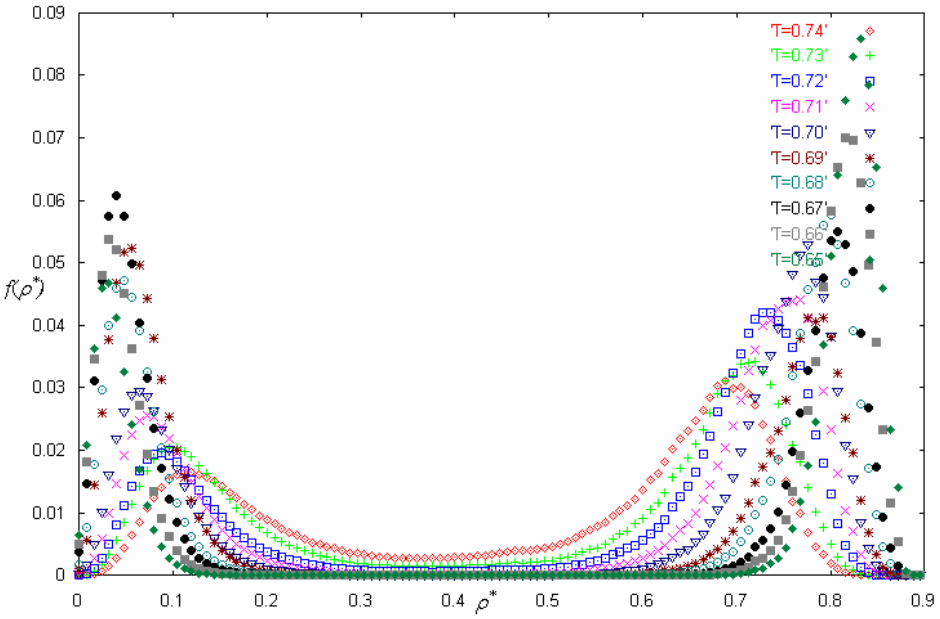

Figure 2: Density Histograms *f(ρ*)* at equilibrium for SW fluid with λ=1.25 obtained from grand canonical simulations

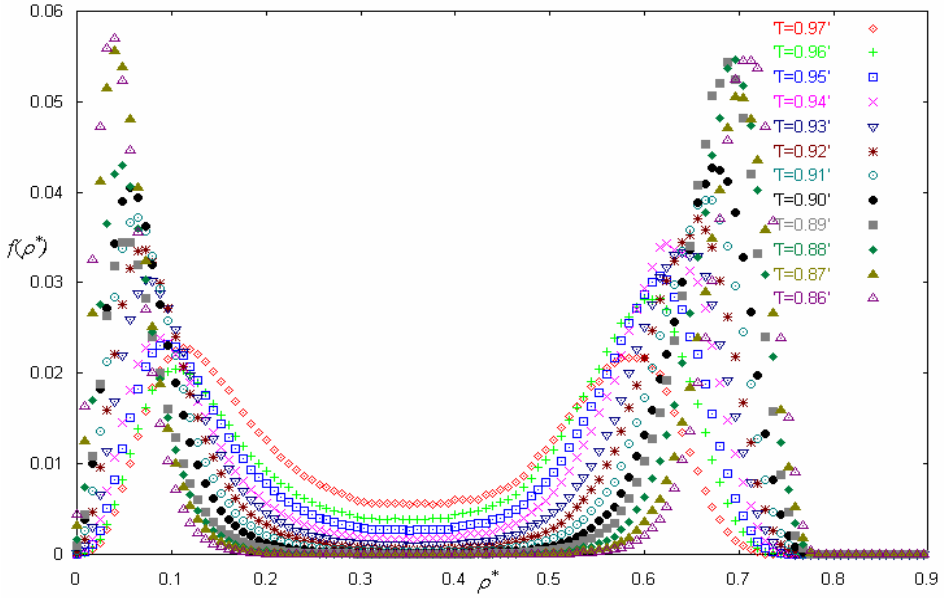

Figure 3: Density Histograms *f(ρ*)* at equilibrium for SW fluid with λ=1.375 obtained from grand canonical simulations

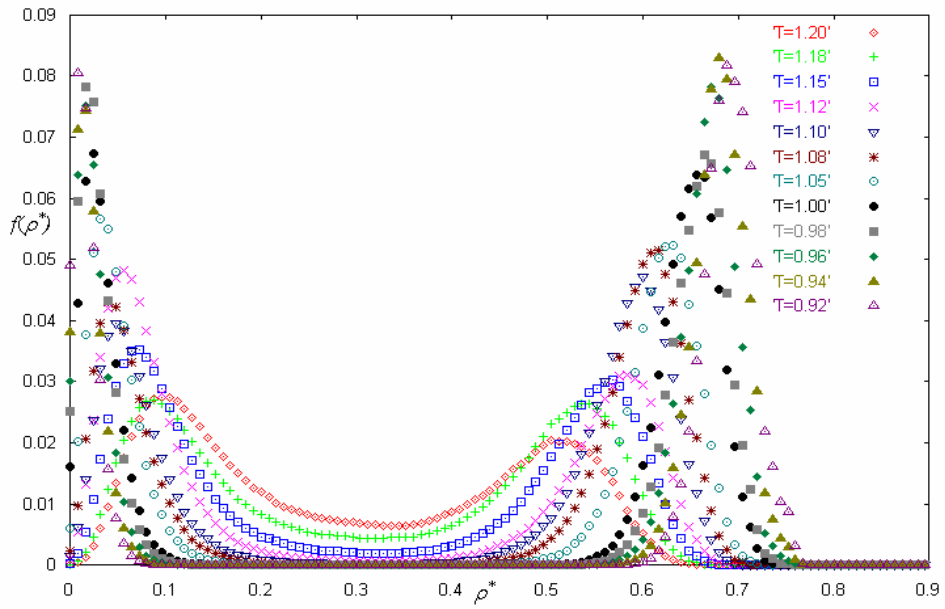

Figure 4: Density Histograms *f(ρ*)* at equilibrium for SW fluid with λ=1.5 obtained from grand canonical simulations

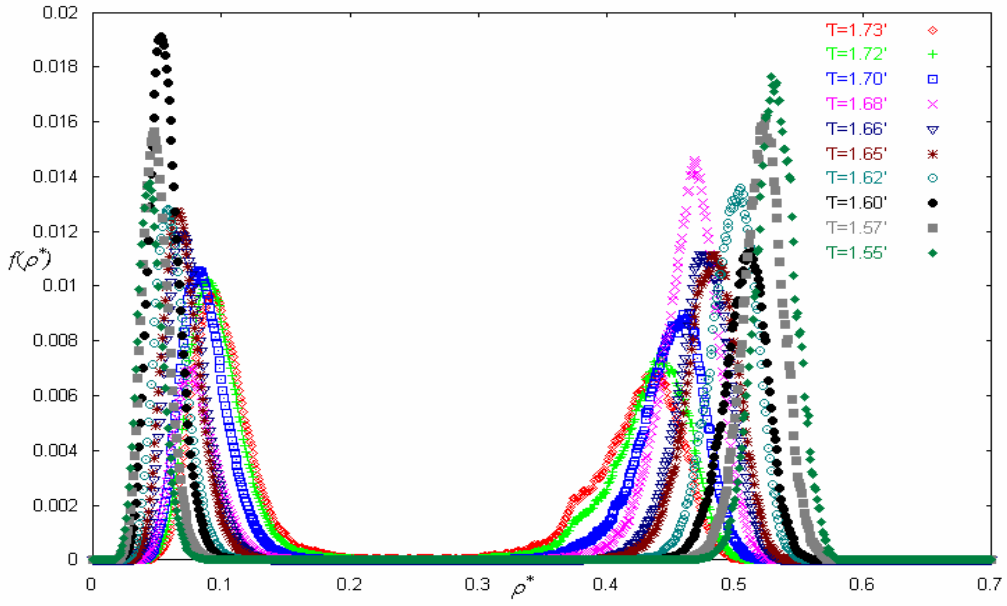

Figure 5: Density Histograms *f(ρ*)* at equilibrium for SW fluid with λ=1.75 obtained from grand canonical simulations

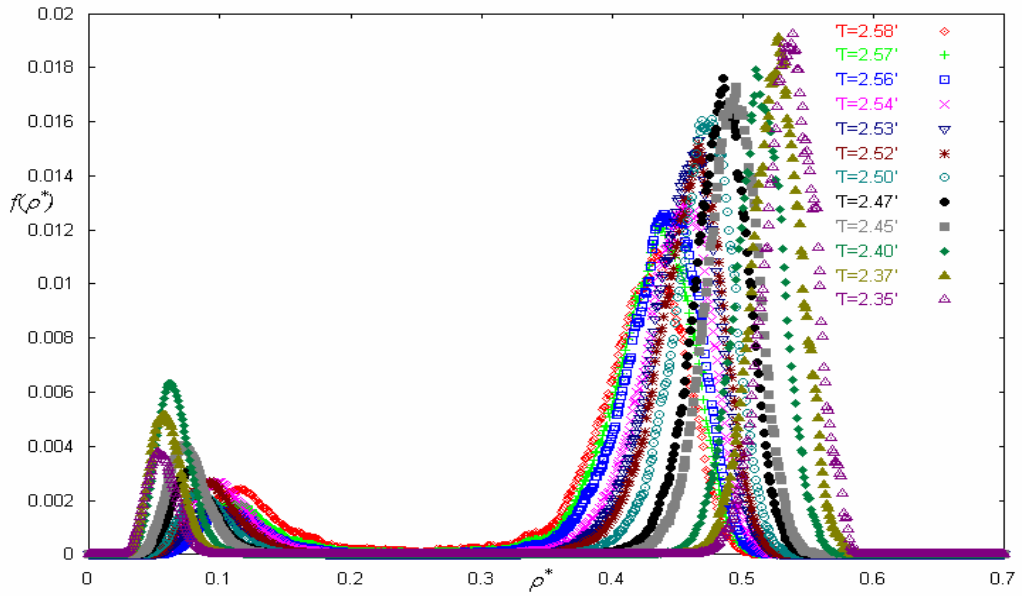

Figure 6: Density Histograms *f(ρ*)* at equilibrium for SW fluid with λ=2.0 obtained from grand canonical simulations

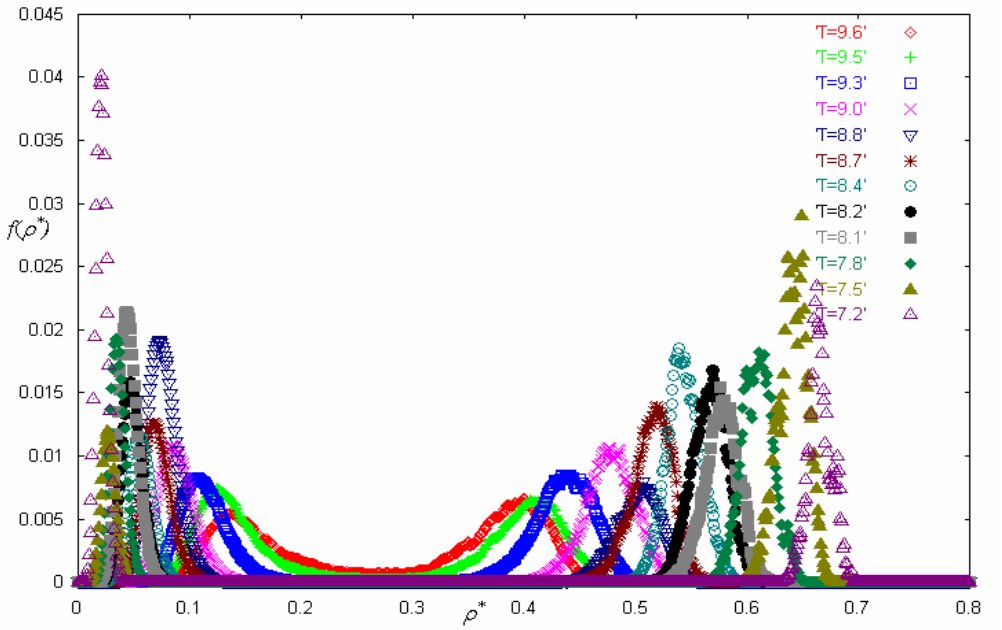

Figure 7: Density Histograms *f(ρ*)* at equilibrium for SW fluid with λ=3.0 obtained from grand canonical simulations

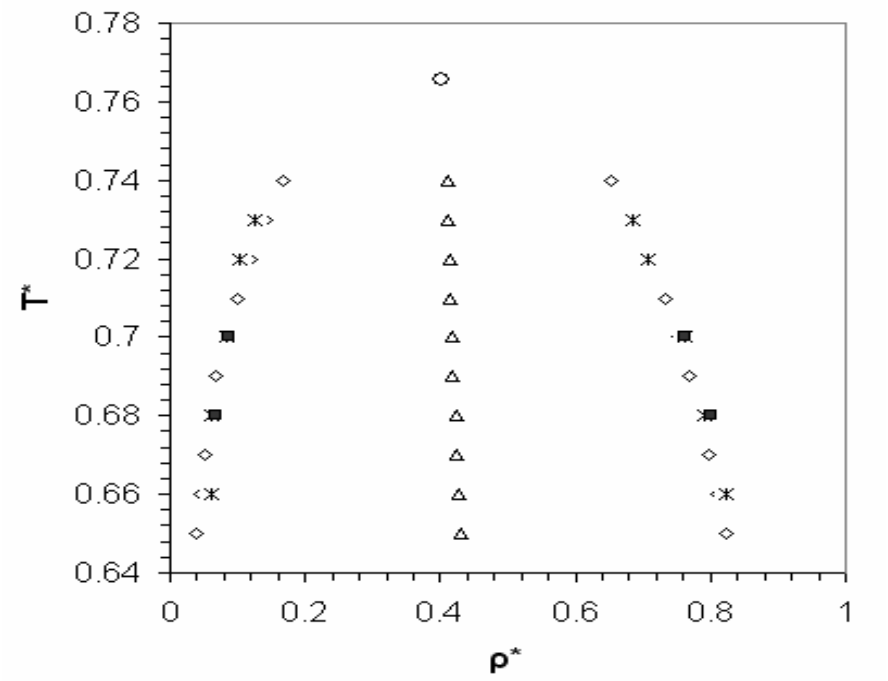

Figure 8: Vapour-liquid T^* versus ρ^* coexistence for SW fluids of range λ = 1.25. ◊, this work; *, Vega *et al.* [18]; ■, Del Rio *et al.* [33]; ○ critical point; Δ lines of rectilinear diameters

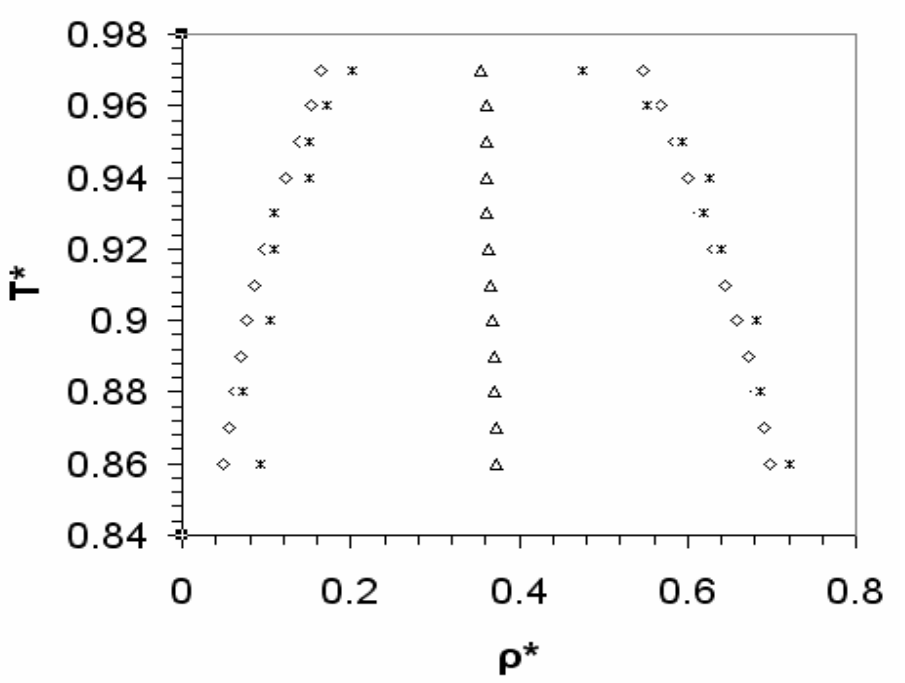

Figure 9: Vapour-liquid T^* versus ρ^* coexistence for SW fluids of range λ = 1.375. ◊, this work; *, Vega *et al.* [18]; ○ critical point; Δ lines of rectilinear diameters

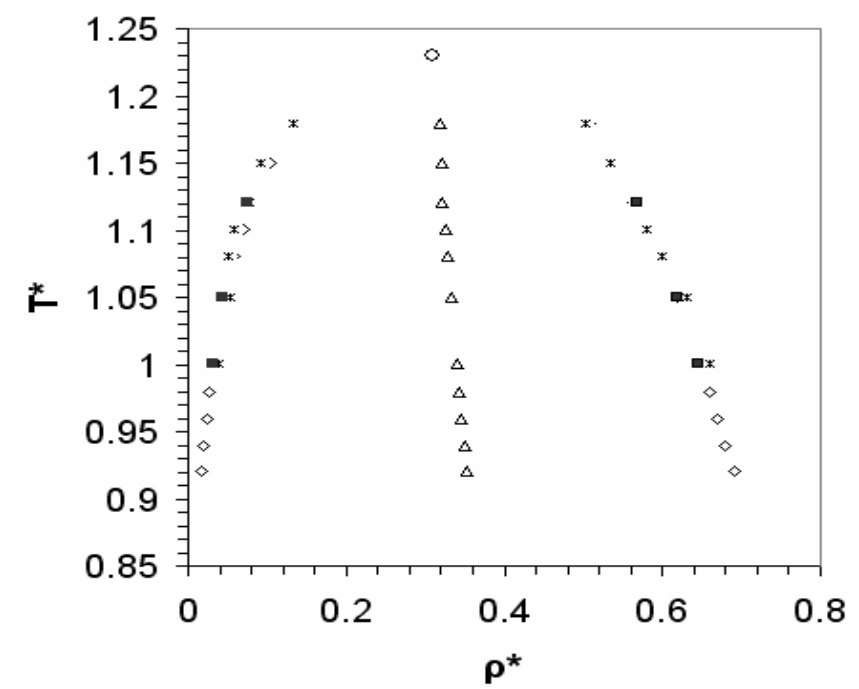

Figure 10: Vapour-liquid T^* versus ρ^* coexistence for SW fluids of range λ = 1.5. ◊, this work; *, Vega *et al.* [18]; ■, Del Rio *et al.* [33]; ○ critical point; Δ lines of rectilinear diameters

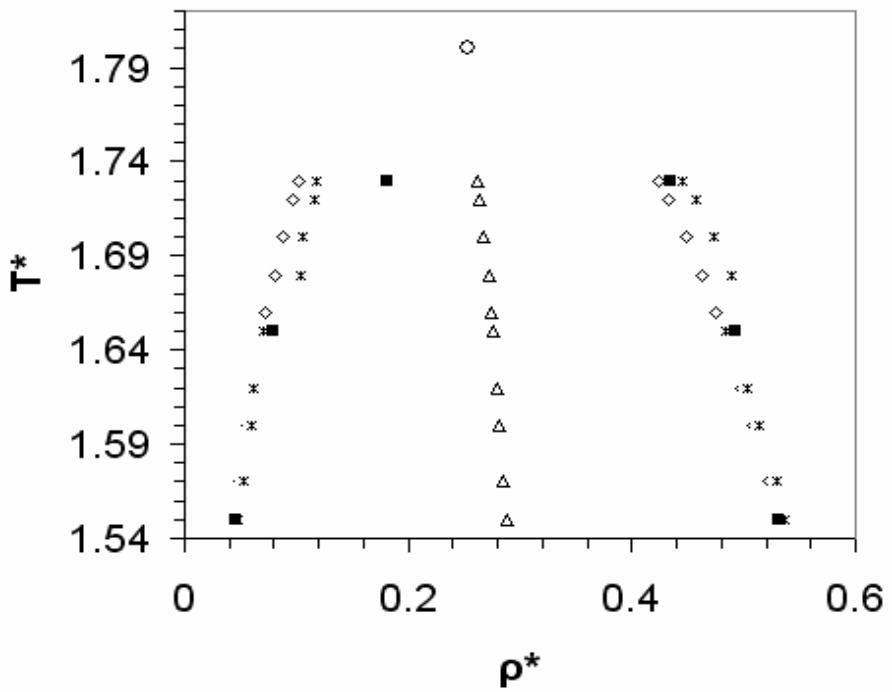

Figure 11: Vapour-liquid T^* versus ρ^* coexistence for SW fluids of range λ = 1.75. ◊, this work; *, Vega *et al.* [18]; ■, Del Rio *et al.* [33]; ○ critical point; Δ lines of rectilinear diameters

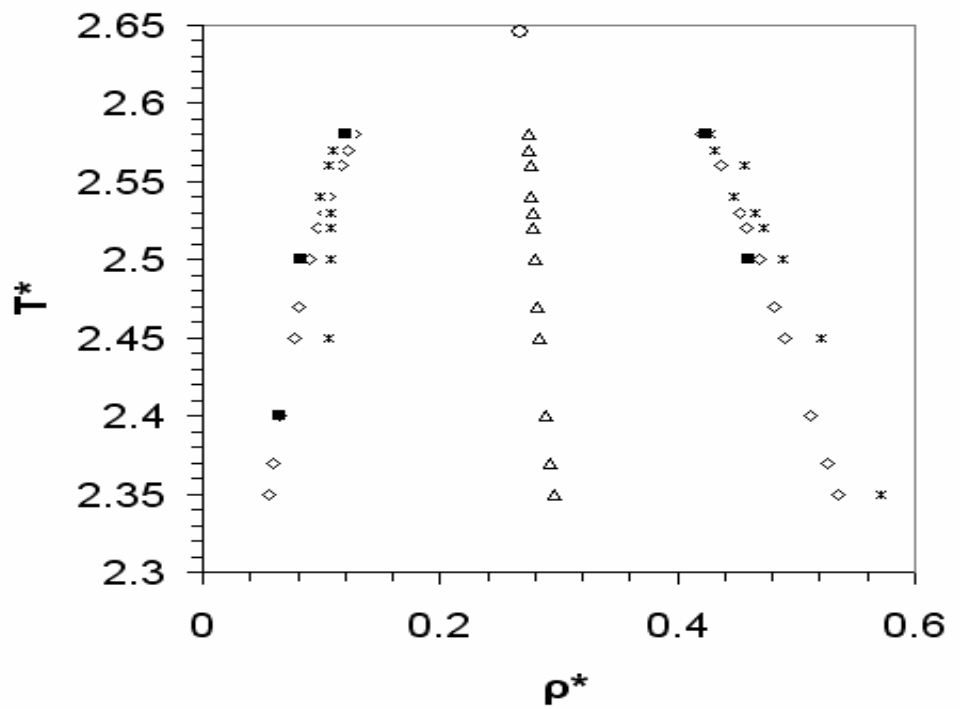

Figure 12: Vapour-liquid T^* versus ρ^* coexistence for SW fluids of range $\lambda = 2.0$. ◊, this work; *, Vega *et al.* [18]; ■, Del Rio *et al.* [33]; ○ critical point; Δ lines of rectilinear diameters

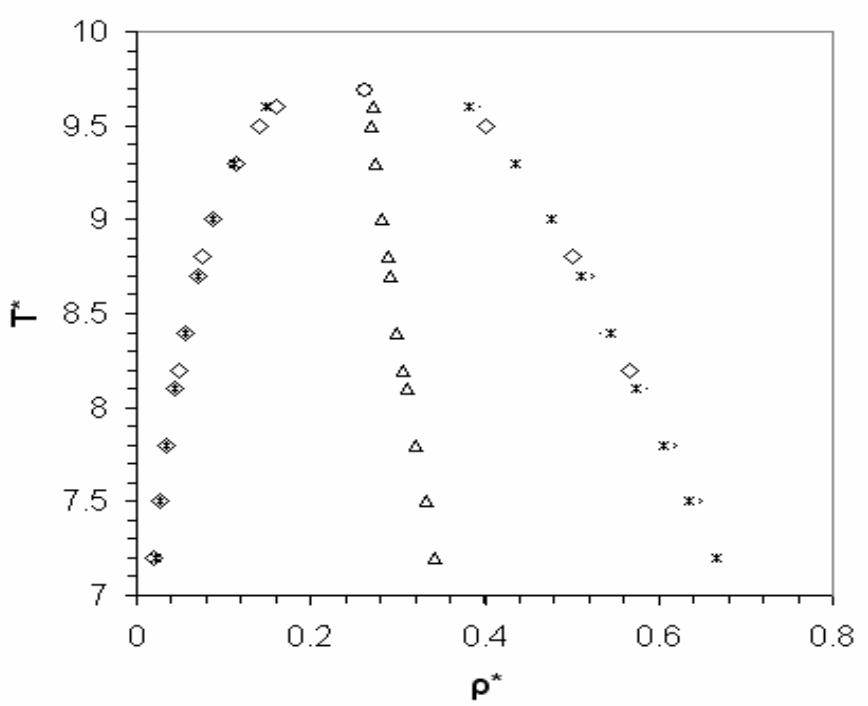

Figure 13: Vapour-liquid T^* versus ρ^* coexistence for SW fluids of range $\lambda = 3.0$. ◊, this work; *, Orkoulas *et al.* [30]; ○ critical point; Δ lines of rectilinear diameters

The values of the critical constants estimated from the simulation data are summarized in Table 1, and a comparison is made with some earlier results. Our results seem to be in somewhat agreement with the earlier reported results [30,33]. The critical temperature and density were estimated by fitting the results to the laws of rectilinear diameters and order parameter scaling [41] with a critical exponent of $\beta = 0.325$. Table 1 also indicate that decreasing λ, i.e. reducing the attractive range, shrinks the range of temperatures for which a stable liquid phase can be found as result of the decreasing critical temperature, T_c.

The lines of liquid-vapour phase co-existence in the space of $\mu^*$and T^* are shown in Figures 14 to 16. The chemical potentials were obtained by implementing the equal peak weight criterion for the density distribution.

Fig. 17 shows the vapor-liquid line with temperatures scaled with the critical temperature T_c of the corresponding range (see Table 1). The lines of rectilinear diameters have also been plotted. This figure gives an excellent view on the effect of decreasing the attractive range on the vapor-liquid equilibria. The figure further shows that the vapor side is hardly affected by the changes in the attractive range. By contrast, a shift towards higher densities is noted on the liquid side of the coexistence curves as the attractive range decreases. For sufficiently short range, the system eventually goes into the solid phase and becomes unstable.

Table 1: Critical properties of the SW fluid with variable range

λ		T_C	ρ_C
1.24	This work	0.7495	0.4084
1.25	This work	0.7657	0.4030
	Vega *et al*. [18]	0.764±0.004	0.370±0.023
	Del Rio *et al*. [33]	0.762	0.3960
1.375	This work	1.2461	0.3112
	Vega *et al*. [18]	0.974±0.010	0.355±0.045
1.5	This work	1.2305	0.3086
	Vega *et al.* [18]	1.219±0.008	0.299±0.023
	Del Rio *et al.* [33]	1.218	0.3016
1.75	This work	1.8003	0.2538
	Vega *et al.* [18]	1.811±0.013	0.284±0.009
2.0	This work	2.6463	0.2675
	Vega *et al*. [18]	2.764±0.023	0.197±0.026
	Del Rio *et al*. [33]	2.691	0.2549
3.0	This work	9.6865	0.2634
	Orkoulas *et al.* [30]	9.87±0.01	0.257±0.001

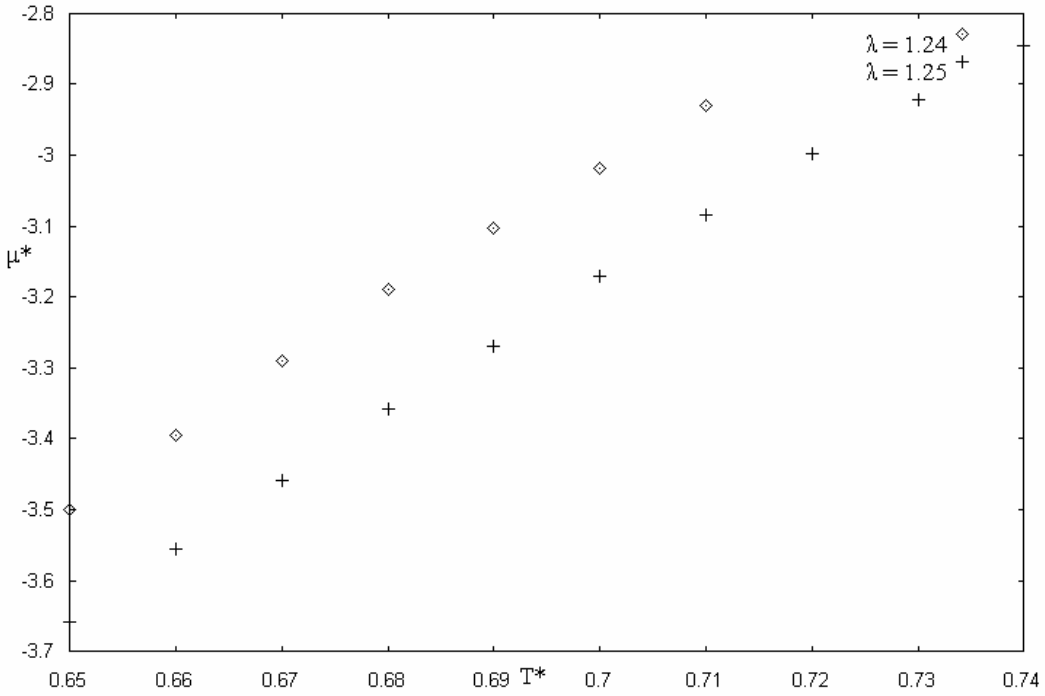

Figure 14: Line of liquid-vapour phase coexistence in μ*-T* space for λ = 1.24 & 1.25

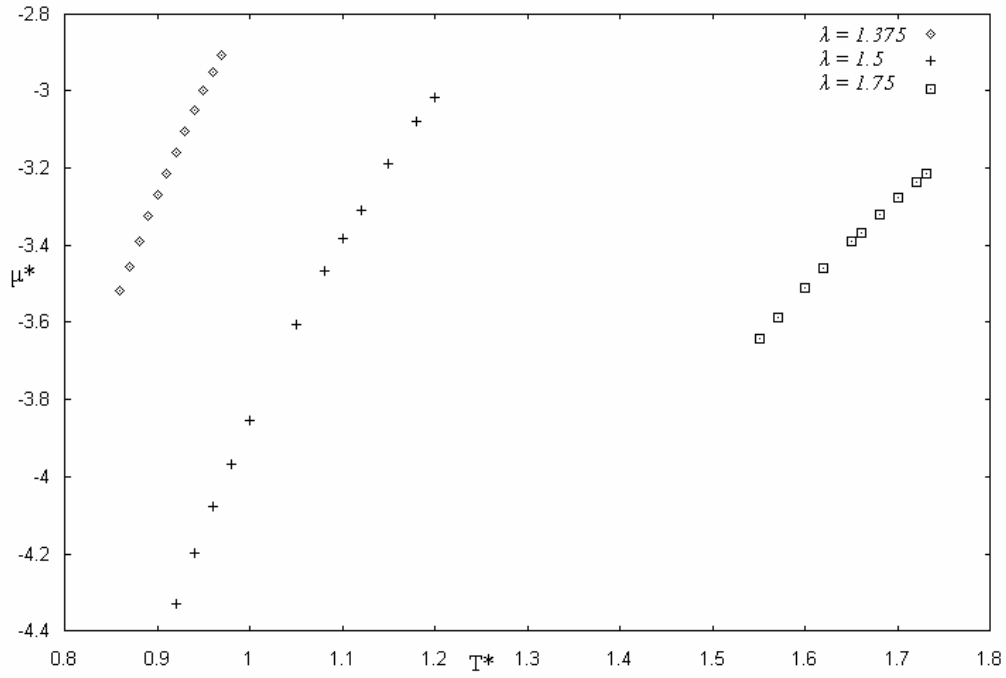

Figure 15: Line of liquid-vapour phase coexistence in μ*-T* space for λ = 1.375, 1.5 & 1.75

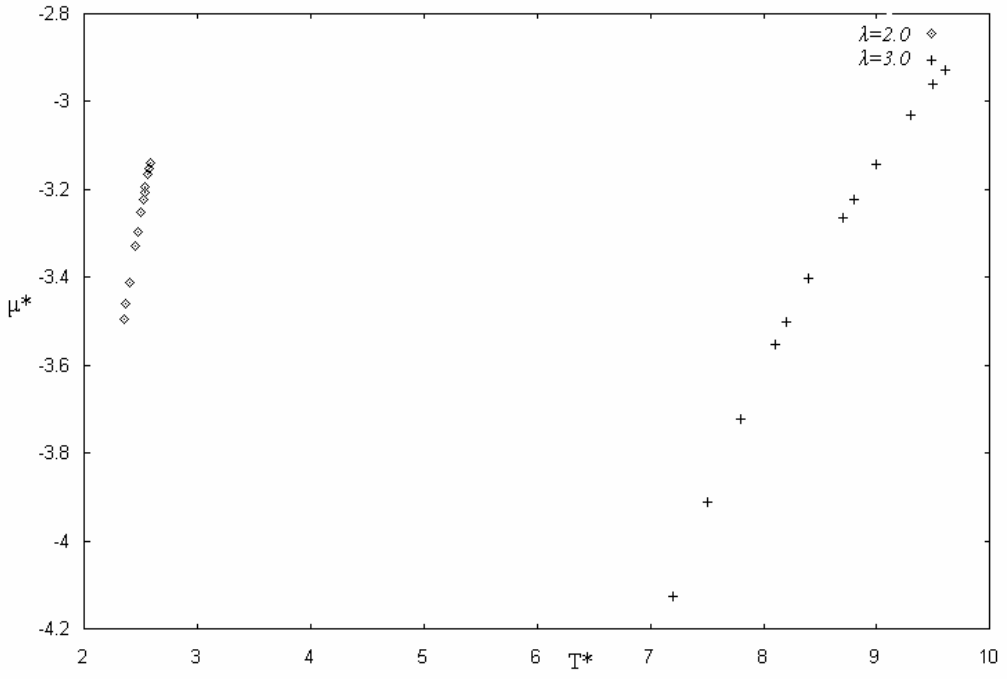

Figure 16: Line of liquid-vapour phase coexistence in μ*-T* space for λ = 2.0 &3.0

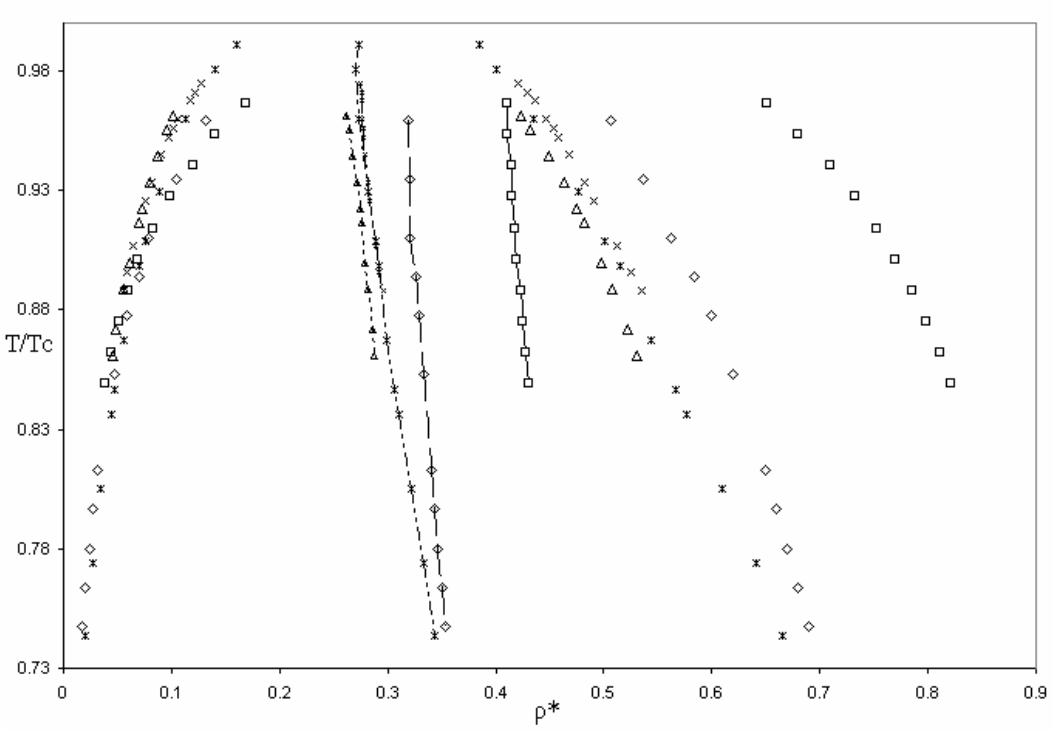

Figure 17: Vapour-liquid coexistence line with temperatures scaled with the critical T_C. Symbols: □, λ = 1.25; ◊, λ = 1.5; x, λ = 1.75; *, λ = 2.0; Δ, λ = 2.0

λ = 1.21 to 1.24

Using the same techniques already outlined for hyper-parallel tempering implemented for grand canonical, simulations were carried out with the view of determining liquid-vapor coexistence for λ range between 1.21 and 1.24.

Figure 18 shows the frequency histogram of densities as determined for square-well with potential range λ = 1.24. The double peak distribution indicates the existence of a two phase region (vapour & liquid). However, after examining a very wide range of temperatures, similar feature (double peaks) was not observed for λ = 1.21, 1.22, and 1.23 as evidenced in Figures 19 to 21. It may therefore be proper to say that λ = 1.24 (not λ = 1.25 which previous theoretical studies showed [37,38,39]), is the threshold value below which liquid phase is not likely to exist.

The coexisting vapor-liquid temperature-density coexistence curves for the SW with potential range λ = 1.24 are shown in Fig. 22. The reduced critical temperature and density have been determined to be 0.7495 and 0.4084 respectively, see Table 1.

The effects of system size have been examined for λ=1.24, very little change was observed in the coexistence densities as the system size was varied from 512 to 2048 atoms, or as the simulation box length was changed to a bigger number. The density histograms for 2048 atoms have been plotted in Figure 23. The histograms are very much like Figure 18 for 512 atoms.

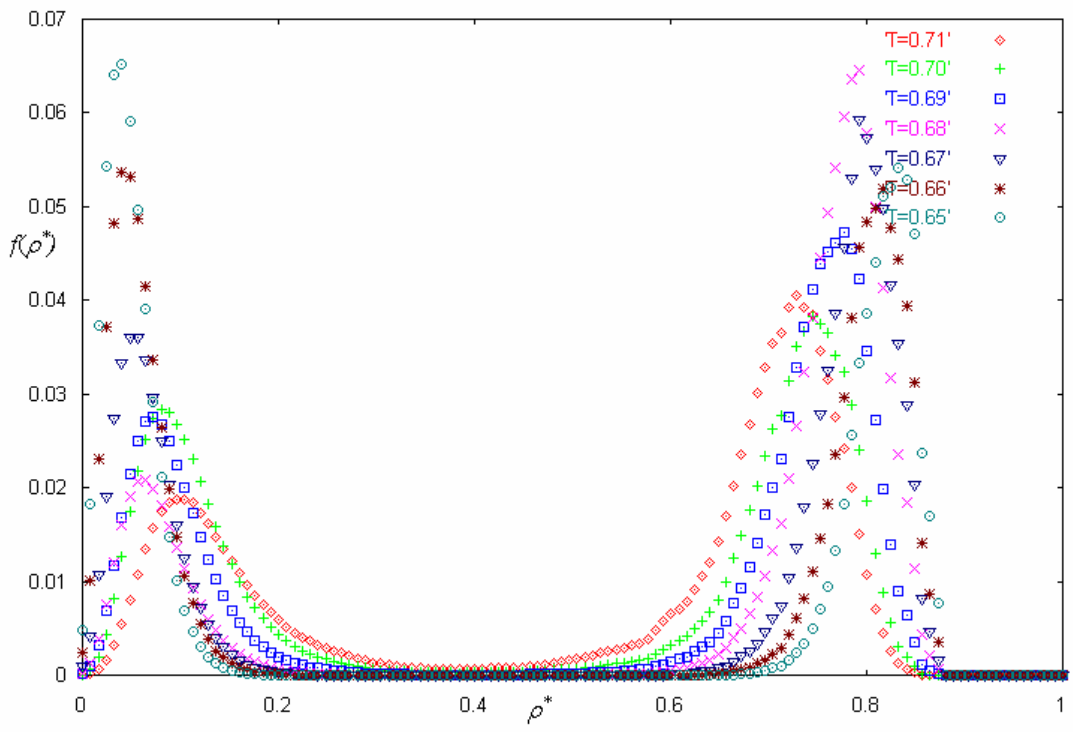

Figure 18: Density Histograms *f(ρ*)* at equilibrium for SW fluid with λ=1.24 obtained from grand canonical simulations

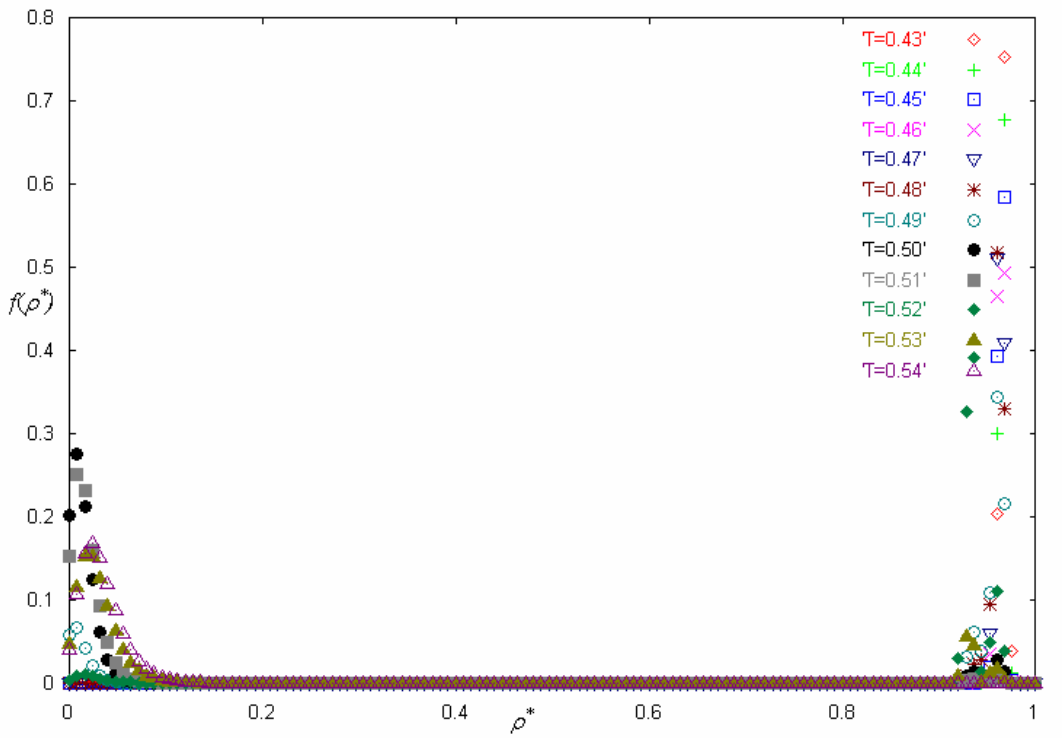

Figure 19: Density Histograms *f(ρ*)* for SW fluid with λ=1.21 obtained from grand canonical simulations. (Double Peaks not observed)

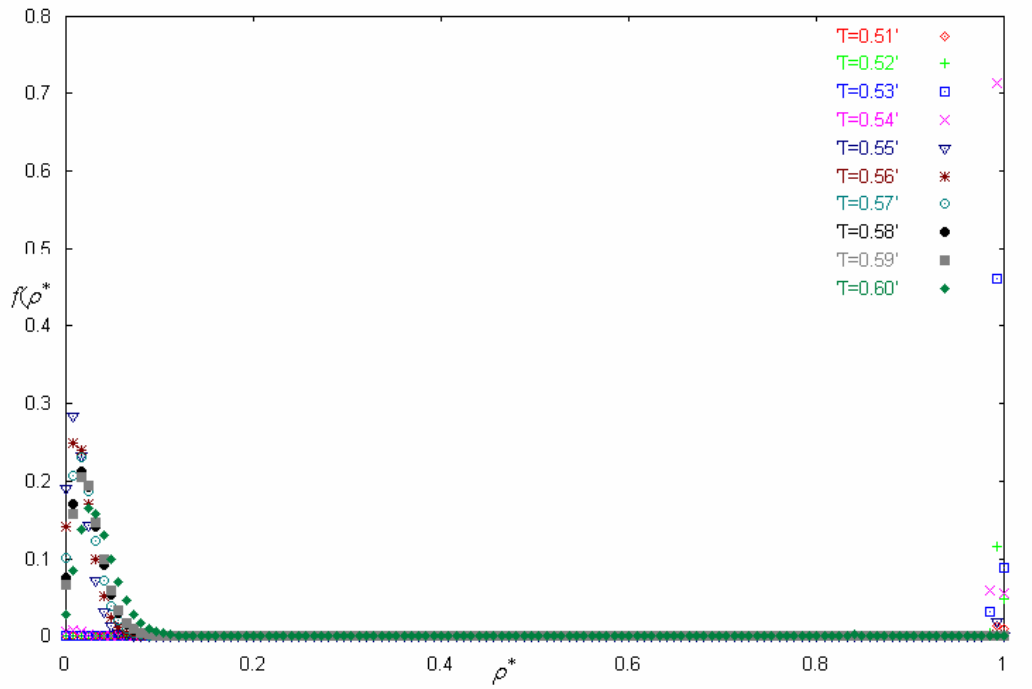

Figure 20: Density Histograms *f(ρ*)* for SW fluid with λ=1.22 obtained from grand canonical simulations. (Double Peaks not observed)

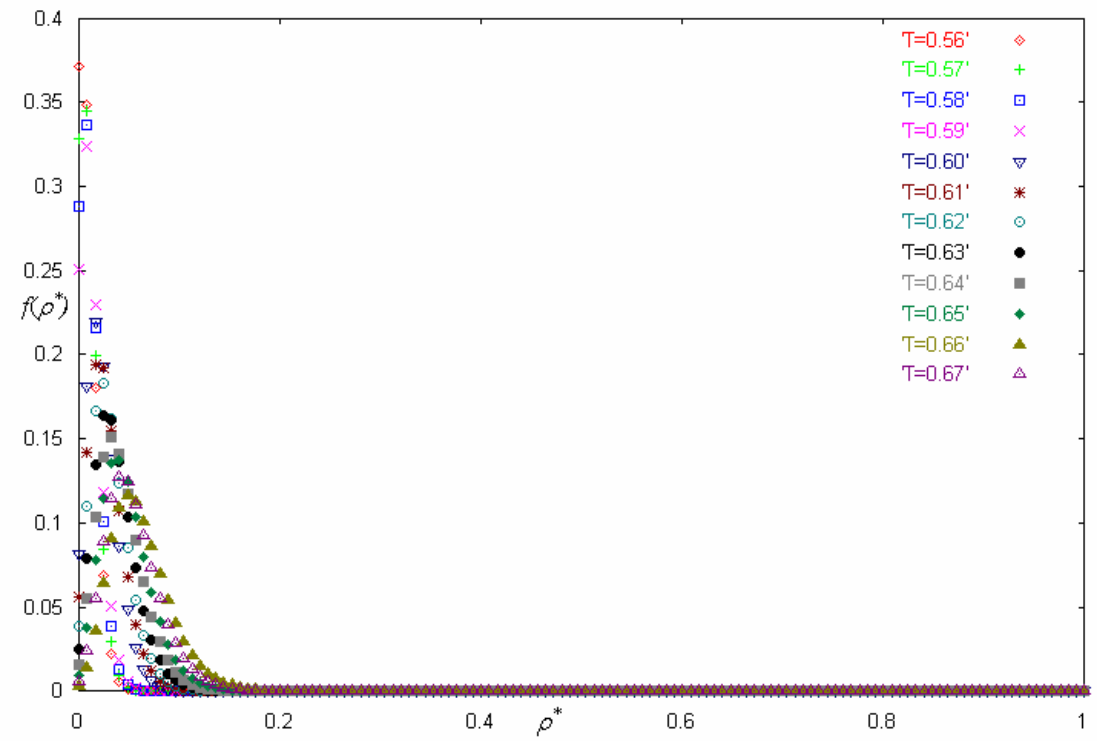

Figure 21: Density Histograms *f(ρ*)* for SW fluid with λ=1.23 obtained from grand canonical simulations. (Double Peaks not observed)

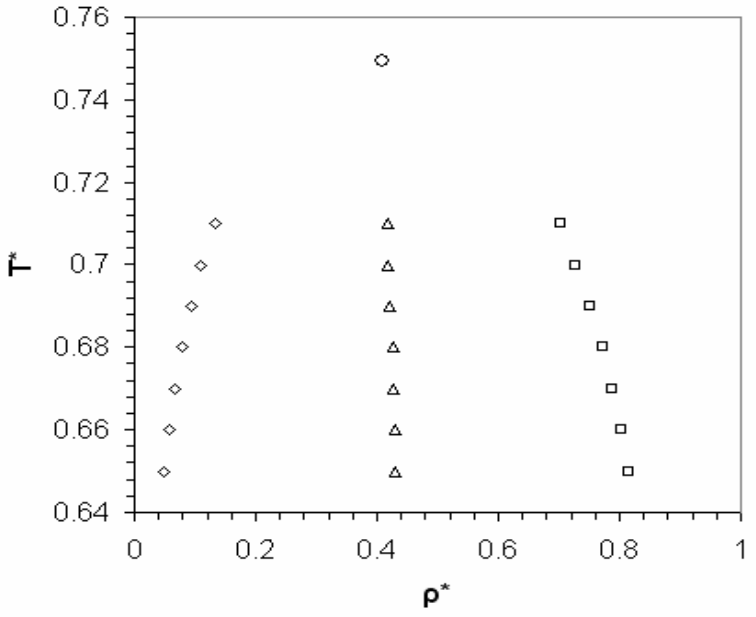

Figure 22: Vapour-liquid T^* versus ρ^* coexistence for SW fluids of range λ = 1.24. ◊, this work; ○ critical point; Δ lines of rectilinear diameters

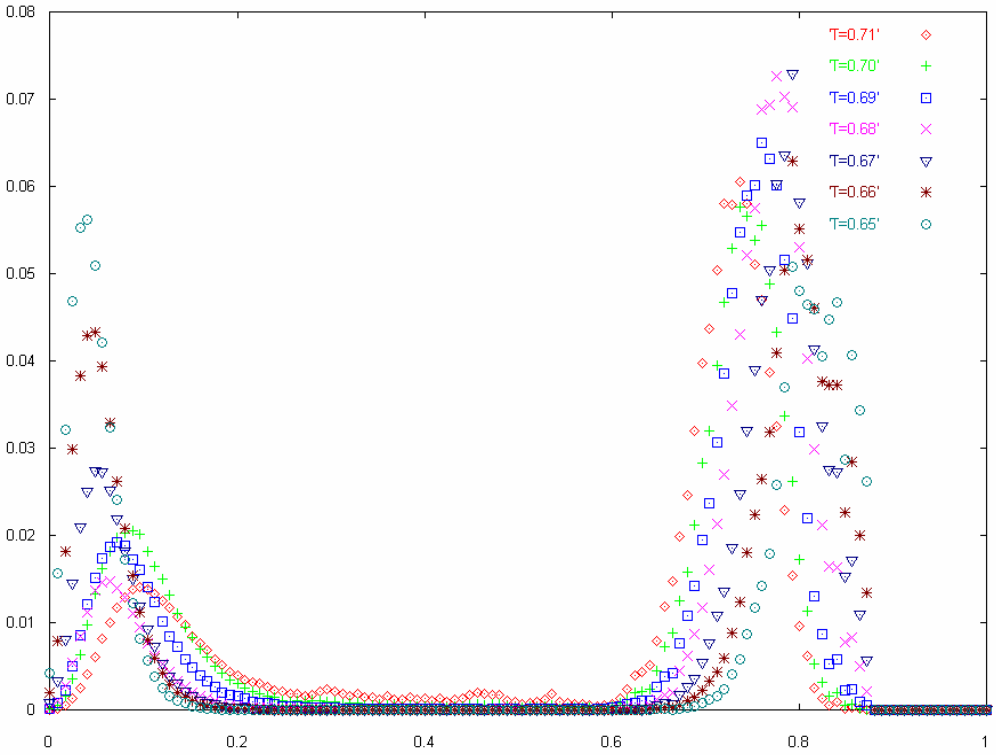

Figure 23: Density Histograms $f(\rho^*)$ at equilibrium for SW fluid with λ=1.24 obtained from grand canonical simulations (2048 atoms)

4. CONCLUSIONS

The hyper-parallel technique of Yang and de Pablo [36] was used in the grand canonical ensemble to determine the phase diagrams of square-well fluids with variable interaction range λ, from 1.21 to 3.0. The grand canonical simulations provided density histograms with double peaked distribution, which is the characteristics of a two phase regime, for potential range λ = 1.24 to 3.0. However, after examining a very wide range of temperatures, similar feature (double peaked distribution) was not observed for λ = 1.21, 1.22, and 1.23. It may therefore be concluded that λ = 1.24 (not λ = 1.25 which previous theoretical studies showed [37,38,39]), is the threshold value below which liquid phase is not likely to exist.

In the analysis of the vapor-liquid curves of square-well fluids with temperatures scaled with the critical temperature T_c of the corresponding range, an excellent view on the effect of decreasing the attractive range on the vapor-liquid equilibria was observed. The analysis shows that the vapor side is hardly affected by the changes in the attractive range. This could be due to the fact that the behaviour is dominated by ideal gas component, given the low densities under consideration. By contrast, a shift towards higher densities is noted on the liquid side of the coexistence curves as the attractive range decreases. And for sufficiently short range, the system eventually goes into high density solid phase and loses stability.

The results of the work clearly indicate that the range of temperatures for which the liquid is stable shrinks as the interaction range decreases. This is because the critical temperature and triple temperature lie closer as λ decrease. And for sufficiently short interaction ranges, both Lennard-Jones and square-well fluids have no stable liquid phase.

The effects of system size have been examined in this work. Very little change was observed in the co-existence densities as the number of simulation particles was changed from 512 to 2048 atoms. Similarly, as the simulation box length was changed from $L=7\sigma$ to $L=10\sigma$, changes observed on the coexistence densities were also not significant in the range of temperatures considered in this study. This, therefore, guarantee that the statistical properties obtained in this investigation are reliable.

5. ACKNOWLEDGMENTS

The author would like to thank the King Fahd University of Petroleum & Minerals for support. The author also gratefully acknowledges Dr. Esam Hamad for useful discussions.

---

6. REFERENCES

1. Poon, W., Pusey, P. and Lekkerkerker, H., *Physics World*, pg. 27-32, (April, 1996).
2. Pusey, P. N. Poon, W. C. K., Ilett, S. M. and Bartlett, P. J., *J. Phys.: Condens. Matter* 6, A29 (1994).
3. Leal Canderon, F., Bibette, J. and Biais, J. *Europhys. Lett*. 23, 653 (1993).
4. Gast, A. P., Hall, C. K. and Russel, W. B., *J. Colloid. Interface Sci*. 96, 251 (1983).
5. Asakura, S. and Oosawa, F., *J. Chem. Phys*. 22, 1225 (1954).
6. Hagen, M. H. J., Meijer, E. J., Mooij, G. C. A. M., Frenkel, D. and Lekkerkerker, H. N. W., *Nature* 365, 425 (1993).
7. Girifalco, L. A., *J. Phys. Chem*. 96, 858 (1992).
8. Cheng, A., Klein, M. L. and Caccamo, C., *Phys. Rev. lett*. 71, 1200 (1993).
9. Hasegawa, M. and Ohno, K., *J. Phys.: Condens. Matter*, 9, 3361 (1997)
10. Mederos, L. and Navascues, G. J., *J. Chem. Phys*. 101, 9841 (1994).
11. Caccamo, C., Costa, D. and Fucile, A., *J. Chem. Phys*. 106, 255 (1997); Costa, D., Caccamo, C., and Abramo, M. C., *J. Phys.: Condens. Matter* 14, 2181 (2002).
12. Hagen, M. H. J. and Frenkel, D., *J. Chem Phys*. 101, 4093 (1994).
13. Mederos, L. and Navascues, G. J., *Phys. Rev. B 50, 1301* (1994).
14. Tejero, C. F., Daanoun, A., Lekkerkerker, H. N. W. and Baus, M., *Phys. Rev. Lett*. 73, 752 (1994).

15. Vliegenthart, G. A., Lodge J. F. M. and Lekkerkerker, H. N. W., *Physica A*, 263, 378 (1999).
16. Vliegenthart, G. A. and Lekkerkerker, H. N. W., *J. Chem. Phys.* 112, 5364(2000).
17. Coussaert, T. and Baus, M., *Phys. Rev. E*, 52, 862 (1995).
18. Vega, L., de Miguel, E., Rull, L. F., Jackson, G., and McLure, I. A., *J. Chem. Phys.,* 96, 2296 (1992).
19. Barker, J. A., and Henderson, D., *J. Chem. Phys.*, 47, 2856 (1967).
20. Smith, W. R., Henderson, D., and Murphy, R. D., *J. Chem. Phys.,* 61, 2911 (1974).
21. Henderson, D., Madden, W. G., and Fitts, D. D., *J. Chem. Phys*., 64, 5026 (1976).
22. Smith, W. R., Henderson, D., and Tago, Y., *J. Chem. Phys*., 67, 5308 (1977).
23. Chang, J., and Sandler, S. I., *Molec. Phys.*, 81, 745 (1994).
24. Rotenberg, A., *J. Chem. Phys*., 43, 1198 (1965).
25. Alder, B. J., Young, D. A., and Mark, M. A., *J. Chem. Phys.*, 56, 3013 (1972).
26. Rosenfeld, Y., and Thieberger, R., *J. Chem. Phys*., 63, 1875 (1975).
27. Henderson, D., Scalise, O. H., and Smith, W. R., *J. Chem. Phys.,* 72, 2431 (1980).
28. Lee, Lloyd L., *Molecular Thermodynamics of Nonideal Fluids*, Butterworths, Massachusetts (1988).
29. Brilliantov, N. V., and Valleau, J. P., *J. Chem. Phys*., 108, 1115 (1998).
30. Orkoulas, G., and Panagiotopoulos, A. Z., J. Chem. Phys., 110, 1581 (1999).
31. Elliot, J. R. and Hu, L. G., *J. Chem. Phys.*, 110, 3043 (1999).
32. Kiselev, S. B., Ely, J. F., Lue, L., and Elliot, J. R., *Fluid Phase Equil*., 200, 121 (2002).
33. Del Rio, F., Avalos, E., Espindola, R., Rull, L. F., Jackson, G., and Lago, S., *Molec. Phys*., 100, 2531 (2002).
34. Orea, P., Duda, Y., Weiss, V. C., Schroer, W., and Alejandre, J. *J. Chem. Phys.,* 120, 11754 (2004).
35. Singh, J. K., Kofke, D. A., and Errington, J. R. *J. Chem. Phys.,* 119, 3405 (2003).
36. Yan, Q. and de Pablo, J. J., *J. Chem. Phys.,* 111, 9509 (1999).
37. Daanoun, A., Tejero, C. F., and Baus, M. *Phys. Rev.* E 50, 2913 (1994).
38. Rascon, C., Navasques, G., and Mederos, L., *Phys. Rev*. B 51, 14899 (1995).
39. Asherie, N., Lomakin, A., and Benedek, G., *Phys. Rev. Lett.* 77, 4832 (1996).
40. Heyes, D. M., *The Liquid State, Application of Molecular Simulations*, John Wiley, England (1998).

41. Frenkel, D. and Smit, B. *Understanding Molecular Simulation: From Algorithm to Applications*, Academic Press, San Diego, (1996).